

# HYBRID SEVEN-BEND-ACHROMAT LATTICE FOR THE ADVANCED PHOTON SOURCE UPGRADE\*

M. Borland, V. Sajaev, Y. Sun, A. Xiao, ANL, Argonne, IL 60439, USA

## Abstract

A hybrid seven-bend-achromat lattice has been designed for the APS upgrade. We describe the design goals, constraints, and methodology, including the choice of beam energy. Magnet strength and spacing is compatible with engineering designs for the magnets, diagnostics, and vacuum system. Dynamic acceptance and local momentum acceptance were simulated using realistic errors, then used to assess workable injection methods and predict beam lifetime. Predicted brightness is two to three orders of magnitude higher than the existing APS storage ring. Pointers are provided to other papers in this conference that cover subjects in more detail.

## INTRODUCTION

The Advanced Photon Source [1] is a 7-GeV, 100-mA, 40-sector, 3<sup>rd</sup> generation storage ring light source with a 1104-m circumference, providing beams to dozens of insertion device (ID) and bending magnet (BM) beamlines simultaneously. After more than 20 years of operation, a major upgrade of the lattice is under consideration. Since APS is an existing facility, a number of constraints must be imposed on any new lattice; these are described in [2].

The basic goal of the lattice design effort is to provide a much lower beam emittance and ultimately an enhancement of x-ray brightness by more than two orders of magnitude for x-rays above 20 keV. The approach is to use a multi-bend achromat (MBA) lattice [3–6], taking advantage of the  $E^2/M^3$  scaling [7,8] of the natural emittance  $\epsilon_0$  with the beam energy  $E$  and the number of dipoles per sector  $M$ .

After considering various concepts [9–11], it was determined that the ESRF-II “hybrid” concept [11] gave the lowest emittance by a factor of more than two. It also gave sextupoles that are three-to-four times weaker, leading to the adoption of this concept.

APS presently delivers 100 mA in 24 bunches about 75% of the time. For the upgrade, a total current of 200 mA with as few as 48 bunches is required, giving the same single-bunch current of 4.2 mA. The APS MBA lattice has a well-developed impedance model [12] that was used to predict single bunch current limits [13]. It shows that a chromaticity of +5 is needed in both planes to ensure the required single-bunch current.

Bunch-lengthening is important in order to preserve the emittance and improve the Touschek lifetime of low-emittance beams. The APS upgrade will incorporate a higher-harmonic cavity (HHC) for this purpose. Detailed

studies of beam dynamics with the HHC have been performed [14, 15], leading to the conclusion that a bunch duration in excess of 50-ps rms is possible.

## DESIGN METHODS

We started our design by scaling the ESRF-II lattice to the APS number of cells and the cell length. Through an iterative process, we developed a matching command file for elegant [16] that incorporated limitations from magnetic modeling as well as requirements for space between elements to accommodate vacuum and diagnostic components [17]. Owing to the large gradients and sextupole strengths coupled with the short magnet lengths, the equivalent hard-edge magnet strength limits are length-dependent; these limits are incorporated into the matching using fits to data from magnetic modeling [18]. In the early stages, the matching runs also included the overall ring geometry. The matching benefited from use of Pelegant’s parallel simplex optimizer [19, 20],

Wide-ranging tune scans were performed next. For each working point, we evaluated the dynamic acceptance (DA) and local momentum acceptance (LMA) using Pelegant for a nominal set of magnet errors assuming symmetrically-powered sextupoles. Multi-objective comparison of the results led to selection of a few promising regions, for which a multi-objective genetic algorithm (MOGA, similar to [21, 22]) was applied based on DA and Touschek lifetime [2, 23]. The algorithm was variously allowed to change the lattice linear optics and the sextupoles, with the sextupoles being given a two-sector translational symmetry (making for 12 sextupole families). Linear optics was varied both by high-level linear optics goals (e.g., tunes, maximum beta functions) and separately by direct variation of gradients; the latter seems more effective. Of the several regions explored,  $\nu_x \approx 95.1$  and  $\nu_y \approx 36.1$  yielded the best results. The lattice functions are shown in Fig. 1, while lattice properties are listed in Table 1.

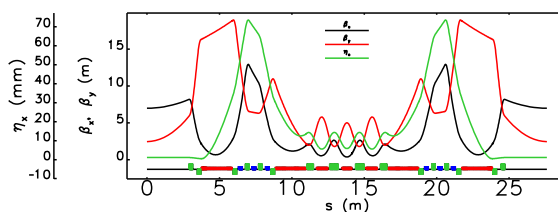


Figure 1: Lattice functions for the APS MBA lattice.

The DA, shown below, is small but suitable for on-axis swap-out injection [24–26]. An alternate lattice supporting accumulation is described in [27]. Figure 2 shows the

\* Work supported by the U.S. Department of Energy, Office of Science, Office of Basic Energy Sciences, under Contract No. DE-AC02-06CH11357.

Table 1: Lattice Parameters

$\nu_{x,y}$	95.125, 36.122	
Natural $\xi_{x,y}$	-139, -108	
Maximum $\beta_{x,y}$	12.9, 18.9	m
Maximum $\eta_x$	0.074	m
Natural emittance	66.9	pm
Energy spread	0.096	%
x,y,z damping time	12.1, 19.5, 14.1	ms
Energy loss per turn	2.27	MeV
Momentum compaction	$5.7 \times 10^{-5}$	
Circumference	1103.98	
$\beta_{x,y}$ @ IDs	6.97, 2.45	m
$\eta_x$ @ IDs	1.11	mm
Effective emittance @ IDs	67.0	pm

“best” results from the MOGA optimization for the LMA with errors. The LMA exceeds  $\pm 2.5\%$ , in spite of the fact that the horizontal tune crosses the half-integer resonance at about  $+2.1\%$ , as shown in Fig. 3. Detailed tracking studies confirm that this resonance is crossed without beam loss even with large errors, in sharp contrast with results for the present APS lattice. Attempts to reduce the momentum tune footprint resulted in reduced momentum acceptance in the high dispersion areas.

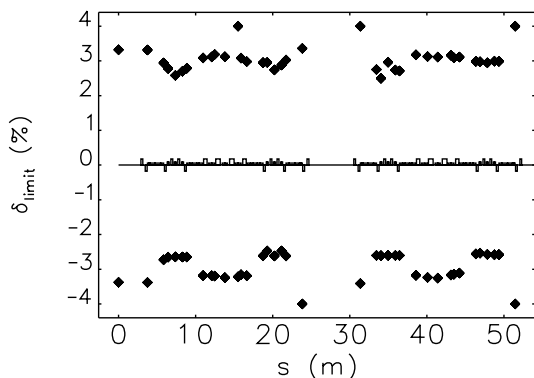


Figure 2: Optimized local momentum acceptance.

## CHOICE OF BEAM ENERGY

The lattice nominally has  $E = 6$  GeV, lower than presently used. Since  $\epsilon_0 \propto E^2$ , even lower energy may be better, particularly if superconducting undulators (SCUs) are employed [28]. However, this scaling is opposed by intrabeam scattering (IBS). We studied energy scaling assuming that the beam current  $I$  varies with energy to maintain fixed rf power delivered to the beam, with 200 mA at 6 GeV as the baseline. Below 4.9 GeV, we capped the current at 500 mA, a plausible limit based on chamber heating considerations. IBS was included using `ibsEmittance` [29], assuming a constant zero-current rms bunch duration of 50 ps and  $\kappa = \epsilon_y/\epsilon_x = 1$ . For a 324 bunch fill, the emit-

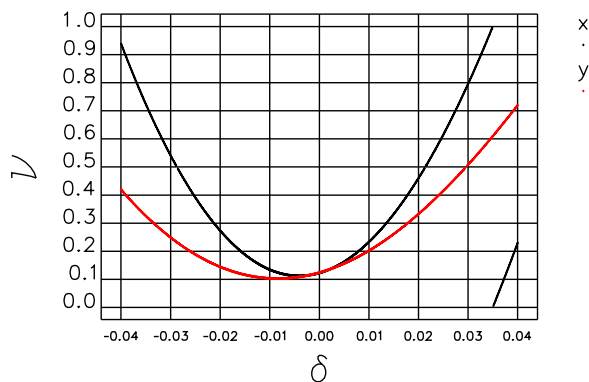


Figure 3: Tunes vs fractional momentum offset.

tance (energy spread) reaches a minimum at about 5.2 GeV (4.9 GeV). The Touschek lifetime drops exponentially with beam energy until the total current limit intervenes at about 4.9 GeV, after which it varies relatively weakly with energy; the beam lifetime at 6 GeV is 2.5 times longer than that at 5 GeV. Figure 4 shows envelopes of x-ray brightness for various beam energies. We see that for 20 keV photons and above, 6 GeV is very competitive with 7 GeV and clearly better than 5 GeV. In addition, 6 GeV is very competitive with 5 GeV for softer x-rays. This comparison is for SCUs, but conclusions are similar for permanent magnet undulators, leading to the choice of 6 GeV as the beam energy.

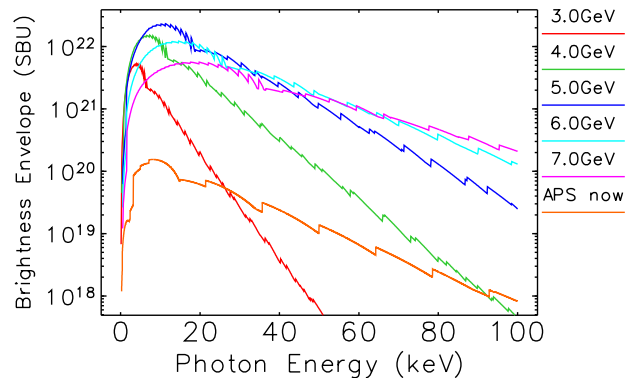


Figure 4: Brightness envelopes for 3.7-m-long SCUs, for various electron beam energies.

## ENSEMBLE EVALUATION

The MOGA optimization includes lattice errors and apertures, so it should provide a robust solution. However, verification is necessary using additional error ensembles. In addition, tolerances on multipole errors in the magnets need to be established and options for ID chamber apertures need to be explored. (By default, elliptical ID chambers with 20-mm by 6-mm major axes are included.) Generation of the error ensembles relies on a simulated commissioning procedure [30], the end result of which is an SDDS file providing a series of configurations, including magnet strength errors, magnet misalignments, steering corrector strengths,

Content from this work may be used under the terms of the CC BY 3.0 licence (© 2015). Any distribution of this work must maintain attribution to the author(s), title of the work, publisher, and DOI.

and skew quad strengths. Using these configurations, after first moving the tunes to the coupling resonance, the lattice functions, beam moments, DA, and LMA are computed using `elegant` and `Pelegant`.

The DA results are post-processed to find percentile contours, as seen in Fig. 5, which shows the 10<sup>th</sup>-percentile contours. (I.e., 90% of the DA results are outside the indicated boundary.) The rms beam size from the APS booster is expected to be 0.65 mm (horizontal) by 0.20 mm (vertical), which is small compared to the DA. Detailed simulation of injection [31] confirms the expectation of high efficiency on-axis injection.

The effects of multipole errors are modest. Also, using a round ID chamber with an 8-mm inside diameter has no significant negative effect. This permits use of horizontal-gap planar IDs [32] and helical superconducting IDs [33], neither of which is easily compatible with accumulation.

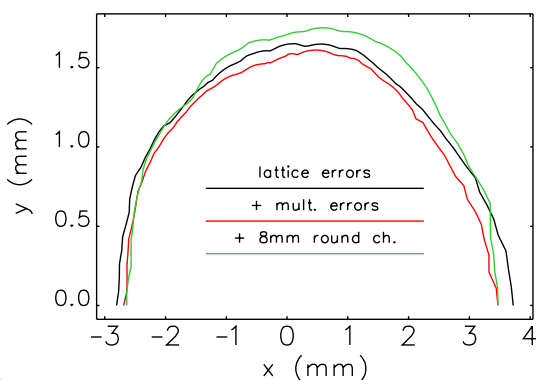


Figure 5: 10<sup>th</sup>-percentile DA contours, including elliptical ID chambers with 20-mm (x) and 6-mm (y) major axes.

Starting from the coupled-lattice emittances, IBS effects were estimated using `ibsEmittance` assuming a 50-ps rms zero-current bunch duration and 200 mA total current. Fig. 6 shows the effects of IBS on the emittance; for comparison, calculations with lower values of  $\kappa$  are also shown. IBS effects are modest for 324 bunches but result in a 50% increase in the horizontal emittance for 48 bunches if  $\kappa = 0.01$  is maintained, while  $\kappa \rightarrow 1$  nearly eliminates this issue.

Using the program `touschekLifetime` [34], the Touschek lifetime was computed using the LMA results from the error ensembles along with the emittances and energy spread from the IBS calculations. As shown in Fig. 7, even for 324 bunches the Touschek lifetime is rather short for low  $\kappa$ , but can be increased considerably by taking  $\kappa \rightarrow 1$ . For 48 bunches, using  $\kappa \approx 1$  is essential to get lifetime over 1 hour. The effect of multipole errors is not negligible; the bulk of the reduction results from random multipoles in the quadrupole magnets, which themselves result from construction errors. More sophisticated lifetime analysis, using computed longitudinal profiles including the HHC and longitudinal impedance, is shown elsewhere [35], but does not show a significant difference. Detailed gas scattering computations are reported in [36].

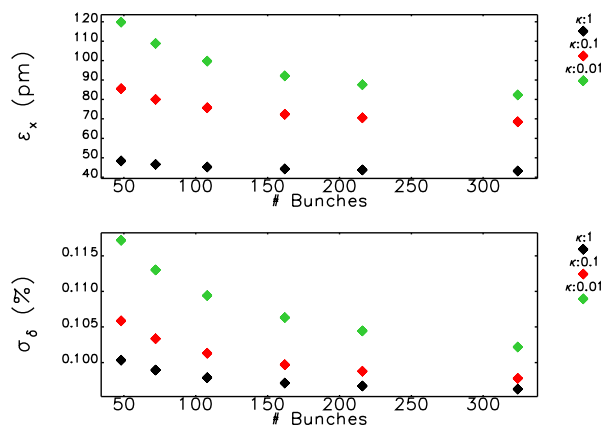


Figure 6: Intrabeam scattering results for 200 mA beam vs number of bunches  $N_b$  and  $\kappa = \epsilon_y/\epsilon_x$ .

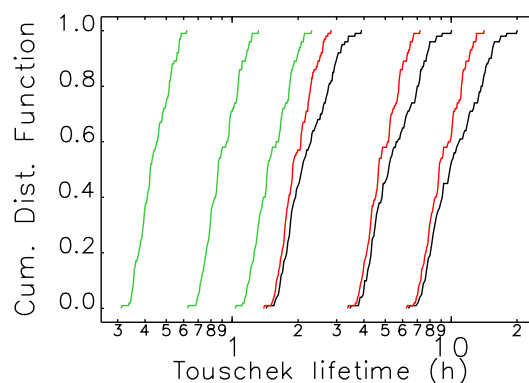


Figure 7: Cumulative distributions of Touschek lifetime based on LMA computed without (black) and with (red, green) multipole errors, for 200 mA in 324 bunches (black, red) and 48 bunches (green). For each color,  $\kappa$  takes values 0.01 (leftmost curve), 0.1 (middle curve), and  $\approx 1$  (rightmost curve).

## CONCLUSIONS

A 6-GeV, 67-pm MBA lattice is proposed as an upgrade for the APS. The design conforms to constraints from magnet designs, vacuum system requirements, and diagnostics requirements. The nonlinear dynamics have been optimized using tracking-based MOGA and evaluated for robustness using 100 error ensembles, including multipole errors and vacuum apertures. The DA is sufficient for on-axis injection, and even 8-mm round ID chambers appear acceptable. Intrabeam scattering and Touschek lifetime are greatly improved by using a large emittance ratio.

## ACKNOWLEDGMENTS

Thanks to: the ESRF-II team for providing their lattice; P. Raimondi for helpful discussion; A. Jain and M. Jaski for multipole error data for magnets. Most computations used the Blues cluster at Argonne's Laboratory Computing Resources Center.

## REFERENCES

- [1] J. N. Galayda. Proc. of PAC 1995, 4–8 (1996).
- [2] M. Borland et al. J Synchrotron Radiation, 21:912 (2014).
- [3] D. Einfeld et al. NIM-A, 335:402 (1993).
- [4] W. Joho et al. Proc. of EPAC 94, 627–629 (1994).
- [5] D. Einfeld et al. Proc. of PAC 95, 177–179 (1995).
- [6] D. Kaltchev et al. Proc. PAC95, 2823–2825.
- [7] J. Murphy. BNL-42333, BNL (1989).
- [8] H. Wiedemann. Particle Accelerator Physics II. Springer, Berlin (1999).
- [9] S. C. Leemann et al. Physical Review ST Accel Beams 12:120701 (2009).
- [10] L. Liu et al. Proc. of 2013 IPAC, 1874 (2013).
- [11] L. Farvacque et al. Proc. of 2013 IPAC, 79 (2013).
- [12] R. R. Lindberg et al. TUPJE078, IPAC15, these proceedings.
- [13] R. R. Lindberg et al. TUPJE077, IPAC15, these proceedings.
- [14] M. Borland et al. MOPMA007, IPAC15, these proceedings.
- [15] L. Emery et al. TUPJE065, IPAC15, these proceedings.
- [16] M. Borland. ANL/APS LS-287, Advanced Photon Source (2000).
- [17] B. Stillwell et al. Private communication.
- [18] M. Jaski. Private communication.
- [19] Y. Wang et al. Proc. of PAC 2007, 3444–3446 (2007).
- [20] Y. Wang et al. Proc. of PAC 2011, 787–789 (2011).
- [21] K. Deb et al. IEEE TEC, 6:182 (2002).
- [22] I. Bazarov et al. Phys Rev ST Accel Beams 8:034202 (2005).
- [23] M. Borland et al. ANL/APS/LS-319, APS (2010).
- [24] E. Rowe et al. Part Accel, 4.
- [25] R. Abela. Proc. EPAC 92, 486–488 (1992).
- [26] L. Emery et al. Proc. of PAC 2003, 256–258 (2003).
- [27] Y. Sun et al. TUPJE071, IPAC15, these proceedings.
- [28] J. Bahrtdt et al. Journal of Physics, 425:032001 (2013).
- [29] M. Borland et al. Proc. of PAC 2003, 3461–3463 (2003).
- [30] V. Sajaev et al. MOPMA010, IPAC15, these proceedings.
- [31] A. Xiao et al. TUPJE075, IPAC15, these proceedings.
- [32] E. Gluskin. TUXC1, these proceedings.
- [33] Y. Ivanyushenkov. Proc. of IPAC14, 2050–2052 (2014).
- [34] A. Xiao et al. Proc. of PAC 2007, 3453–3455 (2007).
- [35] A. Xiao et al. MOPMA012, IPAC15, these proceedings.
- [36] M. Borland et al. MOPMA008, IPAC15, these proceedings.